High-energy scattering of atoms and molecules

V. B. Leonas and I. D. Rodionov

Institute of Space Research, Academy of Sciences of the USSR; M. V. Keldysh Institute of Applied Mathematics, Academy of Sciences of the USSR

Usp. Fiz. Nauk **146**, 7–34 (May 1985)

Research on atom-molecule interactions by high-energy scattering (at energies ~ 1 keV) through small angles (10^{-4}–10^{-2} rad) is reviewed. The present state of experimental methods for this research is discussed. Theoretical aspects of research on potential-energy surfaces by means of high-energy scattering are analyzed. The results of recent research are summarized. In particular, there are discussions of research on elastic and inelastic scattering, a new effect (the vibrational rainbow) discovered in the scattering of atom-molecule systems, and measurements of the spectra of the total energy loss. Some possible directions for the further development of experiments are pointed out. Further experimental progress will require the assimilation of laser methods and position-sensitive particle detectors.

TABLE OF CONTENTS

1. Introduction 332
2. Experimental methods for studying high-energy scattering 335
3. Theoretical aspects of research on anisotropic interactions 338
   a) The problem of an analytic description of anisotropic potential-energy surfaces.
   b) Theoretical models for high-energy atom-molecule scattering.
4. Summary of research results on high-energy scattering 341
   a) Elastic and molecular-inelastic scattering. b) The vibrational rainbow in high-energy scattering. c) Measurements of energy-loss spectra.
5. Conclusion 347
References 347

1. INTRODUCTION

Research on atom-molecule collisions utilizing the scattering of beams of high-energy charged and neutral particles through small angles has been pursued vigorously in several laboratories over the past decade. The results which have been obtained substantially improve our understanding of the nature of the interaction of atomic particles in close collisions, and they open up some new opportunities for describing the macroscopic behavior of matter under the extreme conditions which prevail in such close approaches. Our purpose in this review is to discuss the progress which has been achieved and the outlook for further progress in this field.

High-energy scattering is a branch of the physics of atomic collisions devoted to studying atom-molecule scattering on the repulsive branch with the goals of (a) determining the short-range forces involved in interatomic and intermolecular interactions, (b) studying inelastic molecular transitions, and (c) studying nonadiabatic electronic transitions.

The interactions of atoms and molecules with a relative-motion energy not exceeding 10 keV is described at short and intermediate ranges in the Born-Oppenheimer approximation,[1] in which the motion of the electron component of the quasimolecule is assumed to be independent of the motion of the nuclei. The functional dependence of the energy of the quasimolecule on the distance between the nuclei corresponds to a multidimensional potential-energy surface which is, in the interaction of atoms (the simplest case), a function of a single variable: $V(R)$. Corresponding to a given configuration of the nuclei is a set of potential-energy surfaces, one of which describes the ground state of the electron component, while the others describe excited states. Collisional electronic transitions usually occur at fixed positions of the nuclei (the Franck-Condon principle), when the surfaces corresponding to different electronic states of the system come sufficiently close together. The set of potential-energy surfaces corresponding to different electronic states is fundamental information which can be used to describe the dynamic behavior of molecular systems. In turn, this information is a key to a quantitative description, through achievements in statistical mechanics, of a broad spectrum of macroscopic properties of matter in gaseous and condensed phases.

The theory and the computational facilities available today are so powerful that the accuracy of predicted properties is determined exclusively by the accuracy of the data available on the potential.

The forces which act at short range provide the foundation for the predictions of properties of matter under extreme conditions of high temperatures or extremely high pressures and also for describing the behavior of gaseous systems upon a sharp deviation from equilibrium.

Let us examine in slightly more detail the problem of theoretically predicting the properties of matter (the equa-

 0038-5670/85/050332-17$01.80

tion of state) at extremely high pressures, above 1 Mbar. A considerable effort has been made in recent years to study the shock compression of matter. Measurements have been carried out in the submegabar and megabar ranges for many materials (see the bibliography in the review by Bushman and Fortov[2] and in the recent papers by Nellis *et al.*[3] and Kondo and Ahrens[4]). Shock compression is unavoidably accompanied by a pronounced heating of the matter, so that these results can tell us nothing about cold compression. Theoretical models of thermal excitation can be used here, but their accuracy is poorly controllable. There is the interesting alternative of studying cold compression of matter at pressures in the range 1–1000 Mbar through the use of reliable empirical or nonempirical repulsive potentials. This approach should obviously be regarded as a supplement to dynamic methods.

A question of fundamental importance to the description of the properties of condensed media in a highly compressed state is the validity of describing the interactions in terms of a binary interaction, i.e., the validity of ignoring nonadditive effects. The point of view which has emerged from a prolonged discussion of this question in the literature is that the interaction energy of systems of atoms (or molecules) with closed shells can be described in the additive approximation over a broad range of compressions.[5] For molecular systems, anisotropic potentials can be approximated in a certain way by average intermolecular potentials.[6] In principle, the range of applicability of this description can be studied, and nonadditive corrections can be found, by working from data on scattering in composite systems including, for example, van der Waals clusters.

Let us examine compressed Ar and Xe as examples. The binary potentials found for these gases in the experiments of Ref. 7, can be used to calculate an equation of state. Figure 1 shows the results of such calculations of the compressibility of Ar and Xe at $T = 0$ K. In these calculations it was assumed that Ar and Xe form a crystal lattice with a hexagonal close packing. The energy of the crystal, W, is found by summing the binary interactions, and the compressibility is found from the change in the energy upon a change in the volume of the unit cell, v;

$$W = \frac{1}{2} \sum_{i \neq j} V(|\mathbf{R}_{ij}|), \tag{1}$$

$$P = -\frac{dW}{dv}. \tag{2}$$

For these systems we also have results calculated from the Thomas-Fermi model with quantum and exchange corrections.[8] We see that the compression curves calculated by the two approaches agree quite well in terms of both the overall behavior and the absolute values (an essentially complete agreement can be achieved quite easily in Fig. 1 by slightly changing the absolute values of the empirical parameters; such changes would be completely justified in view of a possible systematic error in the measurements[7]).

For the compressibility of Ne, we might note, there is a significant discrepancy with the conventional Thomas-Fermi model with its corrections. There is reason to believe that this discrepancy is not a consequence of ignoring the nonadditive interaction but instead a manifestation of a shell structure of atoms of a material—an effect presently under discussion in the literature.[2]

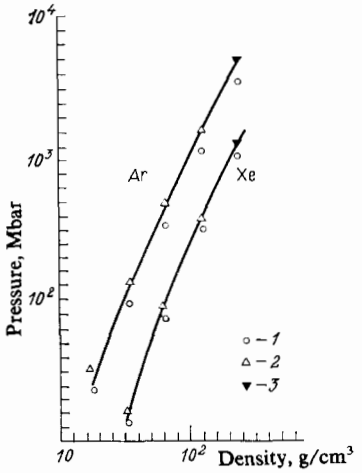

FIG. 1. Curves of cold compression calculated for condensed argon and condensed xenon. Solid lines—Cold-compression curves calculated for a hexagonal close-packed structure of matter through the use of the empirical interatomic potentials from Ref. 7; 1—results of calculations in the Thomas-Fermi approximation with quantum and exchange corrections[8]; 2—data of Ref. 8 after normalization at points labelled 3.

The use of reliable empirical potentials for composite molecular systems (e.g., H_2O, N_2, SiO_2, H_2, and their mixtures) will presumably lead to a reliable prediction of the behavior of matter in the megabar and gigabar pressure ranges.

Theoretical methods are presently the most powerful methods for determining anisotropic potentials, and they will apparently remain so in the future. Progress in computational methods in quantum chemistry and the continuously increasing power of computers have brought us to a stage in which nonempirical numerical calculations of anisotropic potentials have become the primary source of information on potential-energy surfaces.

The number of scientific groups presently carrying out rigorous nonempirical calculations is more than 15 (or more than 20 if we include groups using less rigorous methods).[9] The situation can be illustrated by Table I, which summarizes the systems for which calculations have been carried out on the repulsive anisotropic potentials at energies $\lesssim 10$ eV, with the results frequently in the form of expansions in spherical harmonics. In addition to the systems listed in Table I there have been reports of calculations of the potential surfaces for the following systems (among others): He–H_2O, He–SiO, He–OCS, Ar-OCS, H_2–OCS, H_2–Hcl, H_2–CS, H_2–OH, and Ar–CS_2. Even in the rigorous quantum-chemistry approaches, additional assumptions must unavoidably be used in order to achieve final results of the desired accuracy. It is usually not possible to give a quantitative estimate of the error resulting from these assumptions, so that the validity of the assumptions must be tested independently.

This assertion is particularly pertinent to the approximate approaches, e.g., the model of an electron gas, which has been adopted widely.[10] A basic assumption in this mod-

TABLE I. Summary of theoretical results on the energies of anisotropic interactions

System	Distance range, Å	Energy region, eV; representation used	Reference
	a) Molecular systems		
H_2-H_2	$0{,}8<R<3{,}6,\ r\lessgtr r_e$	$V\leqslant 10$, analytic	11
H_2-CO	$2<R<5,\ r\lessgtr r_e$	$V\leqslant 2{,}5$, graphical, analytic	12, 13
H_2-CO_2	$0{,}8<R<3,\ r=r_e$	$V\leqslant 5$, spline, tabular	14
$HF-HF$	$1<R<3{,}3,\ r=r_e$	$V\leqslant 15$, tabular, analytic	15
N_2-N_2	$1{,}5<R<4{,}6,\ r=r_e$	$V\leqslant 10^2$, analytic	16
H_2O-CH_4	$R<5{,}5,\ r=r_e$	$V\leqslant 1$, analytic	17
CH_4-CH_4	$2{,}6<R<5{,}2,\ r=r_e$	$V\leqslant 1$, analytic	18
	b) Atomic-molecular systems		
$H-H_2$	$0{,}5<R<2,\ r\lessgtr r_e$	$V\leqslant 10$, tabular, graphic	19
$H-CO$	$1{,}6<R<4{,}5,\ r=r_e$	$V\leqslant 1{,}5$ tabular	20
$He-H_2$	$0{,}75<R<10,\ r\lessgtr r_e$	$V\leqslant 10^2$, analytic	21, 22, 23
$He-HF$	$2<R<4,\ r\lessgtr r_e$	$V\leqslant 0{,}5$, tabular	24
$He-LiH$	$1{,}5<R<4{,}5,\ r=r_e$	$V\leqslant 25$, analytic	25
$He-N_2$	$1{,}0<R<2{,}5,\ r=r_e$	$V\leqslant 5$, analytic	26
$He-CO$	$1{,}5<R<6,\ r\lessgtr r_e$	$V\leqslant 15$, analytic, tabular	27, 28
$He-HCl$	$1{,}5<R<4{,}4,\ r=r_e$	$V\leqslant 3$, tabular	29
$He-HCN$	$1{,}7<R<4{,}5,\ r=r_e$	$V\leqslant 3$, tabular	30
$He-CO_2$	$1{,}8<R<4{,}5,\ r=r_e$	$V\leqslant 15$, analytic	31, 32
$He-NH_3$	$1{,}6<R<4{,}8,\ r=r_e$	$V\leqslant 8$, tabular	33, 34
$He-H_2CO$	$1{,}5<R<3{,}5,\ r=r_e$	$V\leqslant 5$, tabular	35
$He-H_2$	$1<R<10,\ r\geqslant r_e$	$V\leqslant 5$, tabular	36
$Ne-H_2$	$1{,}2<R<3{,}2,\ r\lessgtr r_e$	$V\leqslant 5$, analytic	37
$Ne-CO_2$	$1{,}95<R<3{,}5,\ r\leqslant r_e$	$V\leqslant 1$, analytic	38, 39
$Ar-H_2$	$0{,}8<R<3{,}3,\ r\lessgtr r_e$	$V\leqslant 10^2$, analytic	40
$Ar-CO$	$1{,}3<R<4{,}6,\ r=r_e$	$V\leqslant 25$, analytic	41
$Ar-N_2$	$0{,}5<R<8,\ r=r_e$	$V\leqslant 10^2$, tabular	42
$Ar-NO$	$1{,}5<R<4{,}6,\ r=r_e$	$V\leqslant 10$, analytic	43
$Ar-CO_2$	$1{,}8<R<4{,}6,\ r=r_e$	$V\leqslant 15$, analytic	44
$Ar-HF$	$2<R<5,\ r\lessgtr r_e$	$V\leqslant 3$, tabular	24
$Ar-HCl$	$2{,}4<R<4{,}6,\ r=r_e$	$V\leqslant 5$, tabular	45
$O(^3P,\ ^1D)-H_2$	$0{,}3<R<5,\ r\geqslant r_e$	$V\leqslant 3$, tabular	46
$Li-H_2$	$1<R<4,\ r\lessgtr r_e$	$V\leqslant 10$, analytic	47
$He-Na_2$	$2{,}5<R<10,\ r=r_e$	$V\leqslant 1{,}5$, analytic, graphical	48
	c) Ion-molecule systems		
H^+-H_2	$0<R<5,\ r\lessgtr r_e$	$V\leqslant 20$, analytic	49
Li^+-H_2	$1<R<6,\ r\lessgtr r_e$	$V\leqslant 15$, analytic	50
Li^+-N_2	$1{,}5<R<10,\ r\lessgtr r_e$	$V\leqslant 5$, analytic	51, 52
Li^+-CO	$1{,}5<R<10,\ r\lessgtr r_e$	$V\leqslant 5$, analytic	51, 52
H^+-CO	$0{,}9<R<7,\ r\lessgtr r_e$	$V\leqslant 10$, analytic	53
$Li^+(K^+,\ Na^+)-H_2O$	$1{,}5<R<5,\ r=r_e$	$V\leqslant 3$, analytic	54, 55
$He-N_2H^+$	$1{,}8<R<6{,}5,\ r=r_e$	$V\leqslant 10$, tabular	56

el—and the most vulnerable assumption—is that the electron density of the quasimolecule, $\rho(ABC)$, is a linear superposition of $\rho(AB)$ and $\rho(C)$, i.e., the assumption that the electron densities are additive. Over the past few years the electron-gas model has been used to calculate potential-energy surfaces for most of the systems listed in Table I, and we see nothing on the horizon which would prevent a further lengthening of this list. However, in connection with these approximations, both in the rigorous approaches and in the electron-gas model, there is the problem of experimentally testing the reliability of the predictions and possible experimentally based empirical corrections of the approximations (primarily, the approximations of the electron-gas model).

The need for such a test is further motivation for the development of research on high-energy scattering.

In this review we focus on topics *a* and *b* in the second paragraph of this review. We will not discuss the collisional spectroscopy of nonadiabatic transitions.

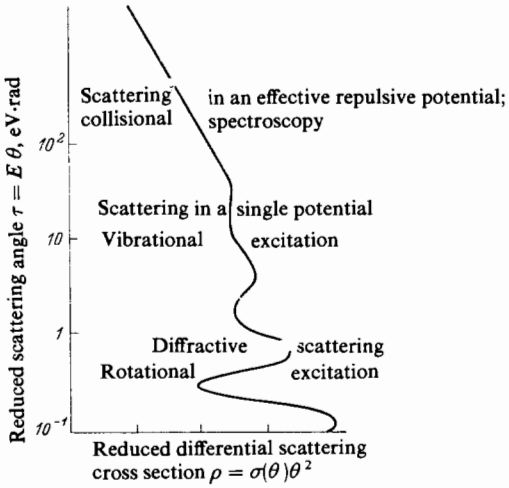

FIG. 2. Characteristic curve of the reduced differential cross section $\rho = \sigma(\theta)\theta^2$; *regions in which the basic effects of small-angle high-energy* scattering are manifested.

2. EXPERIMENTAL METHODS FOR STUDYING HIGH-ENERGY SCATTERING

Since the terms "high energy," "fast beam," etc., are quite arbitrary and frequently provoke subjective associations, we will use the diagram in Fig. 2 to eliminate this arbitrariness. In this diagram the "half-plane" of values of the reduced angle τ ($= E\theta$, where E is the collision energy, and θ is the deflection angle in the laboratory coordinate system) and of the reduced cross section ρ ($= \sigma\theta^2$, where σ is the differential cross section for scattering through an angle θ) is partitioned into overlapping regions in which specific features of high-energy scattering are manifested. These regions are basically the regions which are the subjects of the discussion below. For the conditions in high-energy scattering we can use the estimate $\tau \sim 2V(b)$, where b is the impact parameter, so that the quantity τ specifies the energy of the interaction which causes a scattering of particles through an angle θ in the laboratory coordinate system. It can be seen from this diagram that for the typical case of a beam with an energy of 1 keV the typical high-energy scattering angles lie in the range 10^{-2}–$10°$.

The reason for the upper limit on the reduced high-energy scattering angles is that at larger angles inelastic electronic transitions become comparable to the elastic transitions in the measured scattering cross sections, and the scattering pattern which is observed cannot be interpreted exclusively in terms of one or two intersecting potential-energy surfaces. We might also note that the requirement that the potential-energy surface be unique on the incoming part of the trajectory restricts the study to systems in which the partners have closed electronic shells. The method of high-energy scattering has several advantages for studying the repulsive branch of the potential-energy surface:

1. It is much simpler to produce and detect neutral beams with high energies than with superthermal energies ($\gtrsim 1$ eV).

2. The theory of scattering is immeasurably more transparent and amenable to numerical calculations in the high-energy approximation than at subthermal energies.

3. In high-energy scattering it is simple to achieve approach distances at which electronic terms undergo a quasi-crossing and the transition probabilities are high.

Analysis of the development of research on high-energy scattering reveals several methodological approaches.

The method of integral cross sections can be regarded as historically the first of these approaches. This approach involves measuring the relative intensity of a beam transmitted through a target. The methods for these measurements, which were begun back in the 1940s (Ref. 57), are described in Refs. 58 and 59. They are widely used to determine the short-range potentials of atomic, atom-molecule, and ion-molecule systems.[60,61] The method of integral cross sections has two modifications. Under realistic experimental conditions (the beam, the collision volume, and the detector aperture all have finite dimensions) the flux density of the scattered particles can be resolved into two components, according to Kush[62]: those particles which are scattered and which are removed from the beam detected by the detector and those particles which undergo interactions but remain within the aperture of the detector. The two modifications of the method of integral cross sections involve measurements of both of these components ($-$ and $+$). In the latter case, the particles which have and which have not undergone collisions are distinguished in measurements of the integral cross sections for inelastic transitions by making use of the fact that the inelastically scattered particles acquire an effective "tag" in the form of a change in kinetic energy as a result of the inelastic transition.

The corresponding measured cross sections are described by

$$Q^-(E) = \frac{\Delta I^-}{nI_0L} = 2\pi \int_{(\theta)} \sigma(\theta)\,[1 - f_0(\theta)] \sin\theta\, d\theta, \qquad (3)$$

$$Q^+(E) = \frac{\Delta I^+}{nI_0L} = 2\pi \int_{(\theta)} \sigma(\theta)\, f_0(\theta) \sin\theta\, d\theta, \qquad (3')$$

where $Q^\pm$ is the integral cross section, I_0 is the intensity of the unscattered beam, ΔI^- is the intensity of particles lost from the beam (ΔI^+ is the intensity of the particles which remain within the detector aperture), $\sigma(\theta)$ is the differential cross section for the process in the laboratory coordinate system, $f_0(\theta)$ is the instrumental function,[63] and L and n are the length and density of the scattering target. Under conditions of high-energy scattering the ratio of the total and integral cross sections ($Q/Q^\pm$) can vary from 1 to 3 in different experiments. This variation complicates a direct comparison of the theoretical total cross sections with the measured integral cross sections.

The various types of apparatus for measuring integral scattering cross sections have been described in several places,[59,64] and we will not discuss them further here. We simply note that in the case of ion-molecule systems the development of experimental facilities has taken the path of a significant expansion of the energy range (which now stretches from a few electron volts to a thousand electron volts)[65,66] and an improvement in the resolution of the energy analysis. The best characteristics which have been

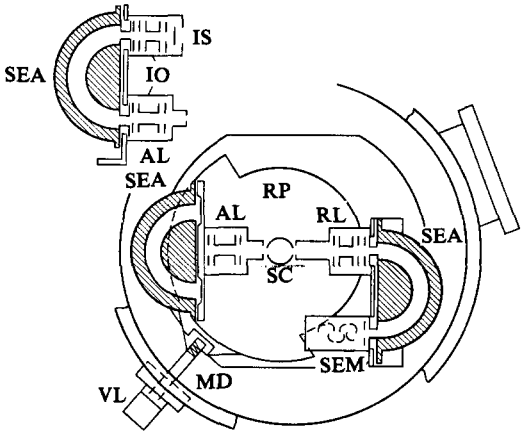

FIG. 3. Apparatus for measuring the integral cross sections $Q^+(E)$ of collisional molecular transitions through an energy analysis of a beam of Li^+ ions passed through the collision chamber.[67] Shown at the upper left is the ion source, with a monochromator selector (rotated 90° with respect to the main diagram). SEA—Spherical electrostatic analyzer; SEM—secondary electron multiplier for detecting the beam; AL, RL—accelerating and retarding Lindholm lenses; SC—scattering chamber; RP—rotating platform for adjustment; MD—mechanical drive; VL—vacuum line; IS—ion source; IO—ion optics.

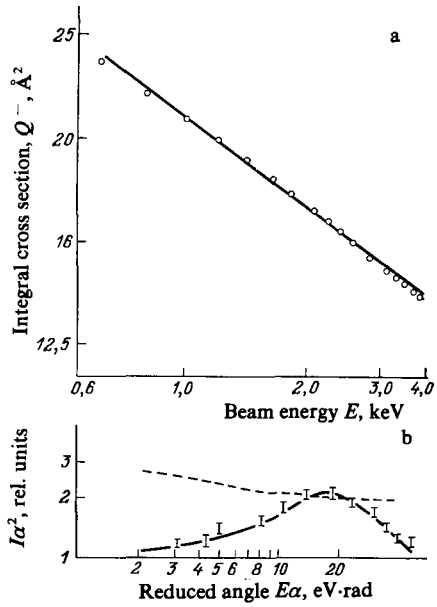

FIG. 4. Results of research on scattering in the N_2–N_2 system. a: Integral cross sections $Q^-(E)$. Solid line—Experimental; circles—calculated on the basis of an additive potential which gives the best fit of the experimental data (the diameter of the circle is 1%). b: Differential scattering. Solid line—experimental; dashed line—calculated with the potential which gives the best fit of the integral cross sections. It is obvious that the differential measurements are more sensitive to the particular features in the behavior of the potential.

achieved to date are those of the apparatus described in Ref. 67 for measuring the cross sections $Q^+(E, \Delta j, \Delta v)$ of collisional transitions between distinct states.

This apparatus is shown schematically in Fig. 1. The basic idea is to measure the intensity of a beam of ions (primarily Li^+) with a given collisional energy loss. Collisional rotational transitions of H_2 and CO_2 molecules[68] and vibrational transitions of N_2, O_2, CO, and other molecules[69] have been studied.

The use of spherical electrostatic energy analyzers in the apparatus shown in Fig. 3 has made it possible to achieve a record high effective resolution. In order to achieve good resolution it is necessary not only to have a high-quality analyzer for the scattered particles but also to have a scattered beam with a very narrow energy spread. These problems are solved by using identical spherical electrostatic analyzers to study the incident beam and to study the beam passed through the target (Fig. 3).

For beams with energies $E \leqslant 200$ eV, a resolution no worse than 10 meV has been achieved in this manner. This high resolution (the relative energy resolution of the selector for an energy $E = 3$ eV was $\Delta E/E = 1/300$) was achieved by first retarding the beam to be analyzed to 3 eV in a retarding electrostatic lens (Fig. 3). The resolution which was achieved made it possible to determine reliably the loss due to collisional excitation and decay of molecular degrees of freedom, e.g., to measure the cross section Q^+ for particular transitions ($j \to j \pm 2$ of molecular hydrogen).

In other studies which have used an energy analysis of ions and neutral particles of a beam,[70,71] the resolution has been substantially worse, and for beams with $E \sim 1$ keV only the loss due to vibrational transitions in the H_2 molecule and due to electronic transitions has been detected.

In evaluating the prospect for the use of the method of integral cross sections we can say that it is an attractive method for measuring the cross sections of transitions which involve a fixed change in the quantum states of the molecules (Q^+), as in Refs. 67 and 72. The use of the method of integral cross sections to study short-range interatomic forces does not seem justified since measurements have shown that the experimental dependence $Q^-(E)$ is only slightly sensitive to the actual potential profile, especially in the case of molecular systems. The situation is illustrated by Fig. 4, which compares measurements and calculations of the integral cross section $Q^-(E)$ and of the angular distribution of the intensity of scattered particles, $I(\alpha)$, for the case of the N_2–N_2 system.[73] We see from Fig. 4 that an additive potential of the exponential type, which gives a good description of the measurements of $Q^-(E)$, is totally incapable of reproducing the pattern of the differential angular scattering. This example, which is not an exceptional case, detracts significantly from the method of integral cross sections $Q^-(E)$ even at the measurement accuracy which has been achieved (1–3%). Nevertheless, measurements of this type continue to be carried out for systems including ions and atoms of inert gases.[74] The limitations of the method of integral cross sections can be overcome by switching to the study of differential cross sections through measurements of the angular distribution of the intensity of scattered particles, $I(\alpha)$, detected by scanning the detector over an angular interval $\alpha = 10^{-3}$–10^{-1} rad. In actual measurements, the detector in angular position α will collect particles scattered through some interval of angles θ.

Figure 5 shows the basic arrangement of an apparatus for differential angular measurements. The measured intensity of scattered particles is related to the cross section by the

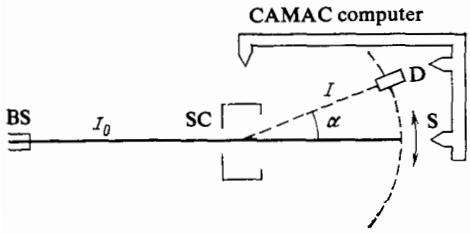

FIG. 5. Schematic arrangement of an apparatus for measuring total integral and differential cross sections for small-angle scattering. The scattered intensities $\Delta I^{\pm}$ measured by a fixed detector and the intensity $I(\alpha)$ of the scattered particles detected by a scanning detector in angular position α are related to the cross sections by Eqs. (3), (3′), and (3″). BS—Source of fast neutral beam; SC—scattering chamber; D—detector; S—drive of system for scanning the detector with respect to the beam axis. The basic components of the apparatus are monitored and controlled by a computer. The computer is coupled to the apparatus through CAMAC apparatus. The computer also performs an initial data processing.[75,122]

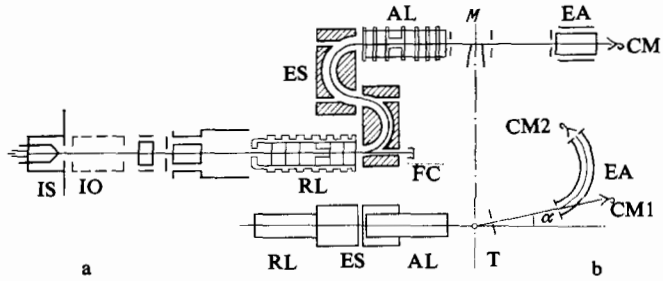

FIG. 6. Apparatus for measuring double differential scattering cross sections.[84] a: IS—Ion source; IO—ion-optics system for formation and mass selection of the beam; RL and AL—retarding and accelerating electrostatic lenses; ES—electrostatic energy selector for the initial beam; EA—scattered-beam energy analyzer; T—target, CM—channel multiplier for detecting the particles; FC—Faraday cup. b: The detection system, rotated 90° with respect to part a of this figure. CM1—Channel multiplier which detects the neutral products of the collisions; CM2—channel multiplier which detects the ion products.

simple expression

$$I(\alpha) = \mathscr{B} \int\limits_{\langle\theta\rangle} \int\limits_{\langle\Omega\rangle} \sigma_\Omega(\theta) f_\alpha(\theta) \sin\theta \, d\theta \, d\Omega, \qquad (3'')$$

where $\mathscr{B}$ is an experimental constant, and $f_\alpha(\theta)$ is an instrumental function for the detector in angular position α—a measure of the efficiency at which the particles scattered through the angle θ are collected. The integration over Ω corresponds to an average over the spatial orientations of the unoriented molecules in the course of the measurements of the cross sections. The width $\langle\theta\rangle$ of the instrumental function, which is bell-shaped,[75] ranges upward from a few milliradians for different pieces of apparatus. This width and, correspondingly, the extent to which the cross sections are averaged in expression (3″) are governed by purely geometric factors (the beam width and the magnitude of the detector aperture). At present the best hope for improving the angular resolution of these measurements is to use position-sensitive detectors made from microchannel plates,[76] which will make it possible to avoid the scanning and (by virtue of the collection of all the scattered particles) will make it possible to speed up the measurements dramatically. An angular resolution as good as 10^{-4} rad may be achieved. Detailed descriptions of various systems of position-sensitive detectors can be found in Refs. 77 and 78. Below we will discuss some results of the measurements which illustrate the actual capability of resolving with their aid the diffraction structure of the differential scattering cross section. The layout of one of the first pieces of apparatus for studying high-energy scattering in the diffraction region was discussed in Ref. 79. There have been several recent reports[80–82] of the use of position-sensitive detectors in research on high-energy scattering.

A natural direction for progress in research on high-energy scattering is to take up measurements of double (angle-energy) differential cross sections. In the case of neutral beams, such measurements could be carried out by an apparatus which performs a time-of-flight analysis of the energy loss (ΔE) of the particles of the scattered beam. For ions, electrostatic analyzers could be used.[83,84]

The apparatus shown schematically in Fig. 6 appears to have the best possibilities among the various systems described in Refs. 83–85. Here a spherical electrostatic selector is used to reduce the energy spread of a primary ion beam extracted from a discharge source. The nominal transmission energy of the selector is 20 eV, and it correspondingly uses a preliminary retardation followed by an acceleration of the selected ions. This approach has reduced the energy spread to no more than 80 meV. An energy analysis of the collision products is carried out with a 127° electrostatic analyzer. Dowek *et al.*[84] state that their apparatus has a working range of 50–1000 eV in terms of the analyzed energy, but the degradation of the resolution at energies above 200 eV causes a serious blurring of the structure in the loss spectrum due to vibrational transitions. For this reason, most of the measurements which have been carried out have dealt with losses due not to molecular transitions but to electronic transitions, in which case the resolution $\Delta E \sim 1$ eV makes it possible to distinguish reliably effects of a transition to excited electronic states.

It should be noted that the method of angular measurements of the loss is in an early stage of development, and only the loss due to electronic excitation of the partners ($\Delta E \gtrsim 1$ eV) can be resolved reliably. Measurements of the double (angle-energy) differential cross sections are complicated by the circumstance that it is necessary to attain high resolution in both of the properties being analyzed—the angle and the energy—while maintaining an adequate signal level. For a beam with an energy of 1 keV, for example, detection of the vibrational structure in the loss spectrum requires a resolution $\Delta E/E$ of about 10^{-4}, which is beyond the capabilities of the time-of-flight method at its present level of sophistication, and is attainable only for the best electrostatic analyzers in the case of ions.

These difficulties in attaining the necessary resolution, which have not yet been overcome, are part of the explanation for the appearance of several studies of quasielastic scattering. In these studies, the angular dependence of the spectrum of the total energy loss (the loss due to elastic scattering and that due to molecular excitation) of fast particles is measured.[86,87]

This discussion of the experimental approaches and the results of a theoretical analysis[88] indicate that any substantial further progress in research on short-range forces will require measurements of the differential cross sections for transitions between distinct levels. Experiments by Bergman *et al.*[89] in the thermal energy region, by laser fluorescence, have shown that it is possible to carry out such measurements and that they are highly sensitive. Measurements of the differential cross sections for rotational transitions are based on the use of laser pumping of the population—a depletion of a selected level—for molecules in the incident beam, followed by detection of the stimulated fluorescence from the same level, populated by collisions involving scattering through a given angle (the double-resonance method). It has been possible to detect the signal produced by a few hundred Na_2 molecules (the corresponding number density in the flux of scattered particles is $n \sim 5 \cdot 10^2$ cm^{-3}). Similar results with respect to detection sensitivity ($n \sim 10^3$–10^4 cm^{-3}) have been achieved for NO. In view of the densities which can be achieved in experiments with high-energy beams, we can expect that corresponding measurements for high-energy scattering will also be successful. The first practical attempt to use the method of induced fluorescence in high-energy scattering was in the experiments of Ref. 90, carried out to determine the rotational-vibrational population both in a beam and in the products of the resonant charge exchange of N_2^+. In these experiments, the energy of the N_2^+ ions in the beam was 800 eV, and this beam was collinear with the light beam from a tunable (pulsed) laser. An important methodological achievement was the reliable detection of a fluorescence signal at a ratio of 10^{16} of the fluxes of primary exciting photons and secondary photons. The signal-to-noise ratio achieved under these conditions makes the outlook for further efforts look promising, although it is clear that the times required to build up the signal in experiments of this sort will unavoidably be long. Use of the laser-fluorescence method requires satisfaction of the following conditions: The molecule must have excited terms to which the molecule can be excited by the light from the tunable lasers available; the lifetime of the excited state must be short enough for convenience in localizing the emission point; finally, the spectroscopic information on the fluorescing molecule must be sufficient for a reliable characterization of the transitions. These conditions are met by, for example, the molecules Na_2, NO, and (in part) SO_2, which are candidates for study in future experiments. Figure 7 is a schematic diagram of a possible apparatus for measurements of the cross sections of $vj \to v'j'$ transitions accompanying high-energy scattering. Here *S* is the source of the monoenergetic fast beam of molecules, which is passed through scattering chamber *SC*; *PuL* is the pump laser, which depletes the vibrational-rotational level selected for the measurements; *PrL* is the probe laser used to determine the change in the population of the pumping level caused by collisions; *M* is a mirror which collects the photons of the fluorescence caused by the probing laser; *PM* is a photomultiplier; and *PSD* is a position-sensitive detector which operates in a particle-(fluorescence photon) coincidence circuit. A unit which selects such coincidences (*PPC*) makes it possible to measure

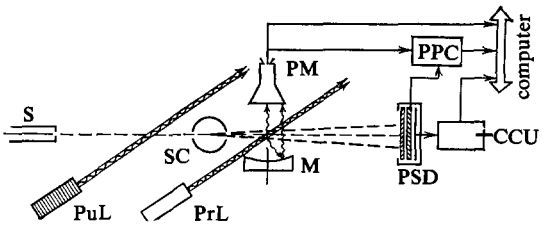

FIG. 7. Arrangement for a possible laser experiment to measure the differential cross section for transitions between distinct vibrational-rotational states. S—Source of fast beam; SC—collision chamber; PrL and PuL—Probing and pumping lasers; M—mirror for collecting fluorescence photons; PM—photomultiplier; PSD—position-sensitive detector; CCU—coordinate calculation unit; PPC—unit for selecting coincidences of a photon with a fast particle; the computer is a control microcomputer.

the cross sections corresponding to transitions to the pumping level, i.e., to measure $\sigma(\Delta v, \Delta j, \theta)$ under conditions of high-energy scattering.

It is attractive to use the double-resonance method in experiments on high-energy scattering, but in the version of the bombardment of a fast beam which we have discussed here the fluorescence signal may turn out to be extremely low because of the low densities and a possibly high rotational temperature of the beam molecules. Perhaps more encouraging is a version in which the steady-state target is replaced by a target consisting of a second intersecting beam. The beam of target molecules can be bombarded by pumping and probing lasers, and the photons of the stimulated fluorescence can be detected in coincidence with the arrival of scattered fast particles at the position-sensitive detector.

By scanning with a laser over the absorption band of the molecules under study one can extract information on transitions between various levels; this would be an extremely informative experiment, and it is a desirable development.

The arsenal of new experimental facilities for studying high-energy scattering thus includes methods of differential scattering (in particular, in the diffraction region), measurements of the energy-loss spectrum, and, finally, the promise of experiments using laser fluorescence.

3. THEORETICAL ASPECTS OF RESEARCH ON ANISOTROPIC INTERACTIONS

a) The problem of an analytic description of anisotropic potential-energy surfaces

In the case of isotropic scattering, even a Lennard-Jones potential will allow a qualitative study of essentially all the features of the scattering. For an anisotropic interaction, on the other hand, we do not yet have a reasonably comprehensive potential with anything in the way of a solid basis, and in practice we use either very simple models or analytic approximations of nonempirical energy calculations. To find such analytic approximations, however, is frequently quite difficult in the repulsive region. For example, an attempt[14] to find an analytic description of interaction energies calculated for 1052 relative positions of H_2 and CO_2 molecules proved unsuccessful, and in Ref. 16 it was not possible to choose an analytic representation for the anisotropic interaction potential of the N_2–N_2 system.

Two types of coordinate systems are used to analyze the interactions of molecules; a spatial coordinate system and a coordinate system moving with a molecule.[91] In nonempirical calculations of interaction energies, which are always carried out for a discrete set of configurations, it turns out to be more compact to use the system which is moving with the molecule, while dynamic calculations are carried out more conveniently in a spatial coordinate system.

The most common representation for the potential-energy surface of the interaction of an atom with a linear molecule is in the molecular coordinate system, with an expansion of the angular dependence in Legendre polynomials:

$$V(R, r, \gamma) = \sum_{l=0}^{L} V_l(R, r) P_l(\cos\gamma), \quad \cos\gamma = \widehat{\mathbf{R}\mathbf{r}}, \tag{4}$$

where r is the radius vector of the internuclear distance in the molecule. The studies are frequently limited to the model of an oscillating rotator in which the expansion of $V_l(R, r)$ in $q = r - r_e$ is cut off at second-order terms (r_e is the equilibrium internuclear distance).

The dependence of the potential-energy surface on the internal coordinates has been analyzed in most detail for the LI^+–N_2 case in a recent paper by Pfeffer and Secrest.[52] They proposed an analytic approximation for the set of interaction energies calculated by Staemler[51] for the Li^+–N_2 system, including a calculation of the dependence of $V_l(R, r)$ on the internal coordinate q.

In some cases, the analyses of effects associated with collisional vibrational transitions are restricted to terms with $l = 0$. This approximation is called the model of a "breathing" or "pulsating" sphere. The quantitative dependence of the potential-energy surface on the internal coordinate q has not received the attention it deserves (as can be seen from Table I above). It is this dependence[92] which, according to our understanding, determines the vibrational rainbow which we will be discussing below.

In the case of interaction of complex molecules, the description of the potential-energy surface becomes extremely complicated, as can be seen from the case of two linear molecules, characterized by orientations $\Omega_{1,2}$ $\{\chi_{1,2}\ \varphi_{1,2}\}$ in the spatial coordinate system.

The potential function $V(R, \Omega_1, \Omega_2)$ can be expanded[93] in a series in orthogonal polynomials in the space $\Omega_1\Omega_2$, and for linear molecules this series is usually chosen as a product of spherical harmonics, $Y_{lm}(\Omega_1)$ and $Y_{l',-m}(\Omega_2)$.

We thus write

$$V(R, \Omega_1, \Omega_2) = \sum_{l, l', m} V_{ll'm}(R)\, Y_{lm}(\Omega_1)\, Y_{l',-m}(\Omega_2). \tag{5}$$

The coefficients $V_{ll'm}(R)$ for the function $V(R, \Omega_1, \Omega_2)$ are calculated from

$$V_{ll'm}(R) = \int\int V(R, \Omega_1, \Omega_2)\, Y^*_{lm}(\Omega_1)\, Y^*_{l',-m}(\Omega_2)\, d\Omega_1\, d\Omega_2. \tag{6}$$

This expansion is of practical interest only if it can be cut off after a few terms.

In the simplest approximation, the energy of the interaction between two molecules can be written as the sum of contributions from binary interatomic interactions—this is the type of empirical surface which corresponds to the model of an additive interaction. The additive model is used extremely widely for describing the interactions of polyatomic systems. It is assumed that a force center (which does not necessarily coincide with the atom) can be associated with each of the atoms of the system, and the interaction energy, e.g., for a system of diatomic molecules AB–CD, is written in the form

$$V(R, r_{AB}, r_{CD}, \Omega) = \sum_{i,j} V(R_{ij}); \tag{7}$$

here R is the distance between the centers of gravity of the molecules, Ω is the set of angular variables describing the relative orientation of the molecules, r_{AB} and r_{CD} are the internuclear distances in the molecules, and R_{ij} is the distance between the force centers of the different molecules. In the case of a repulsive interaction, $V(R)$ is usually approximated by a power law[58] or an exponential law,[59] and the values of the parameters are chosen on the basis of calculations of some measurable quantity [e.g., the integral cross section $Q^-(E)$, which depends on the potential]. The relative simplicity and attractiveness of the additive model for calculating scattering patterns stem from the elimination of the specific angular dependence from the potential-energy surface. It is necessary only to postulate the positions of the force centers in the interacting molecules.

Since the additive model is empirical in nature, there is essentially no experimental way to test it. However, in those cases where there are independent and reliable calculations of interaction energies for various configurations, these results can be compared with the predictions of the additive model. This comparison was carried out for the H_2–H_2 system by McMahan *et al.*,[94] who found that the additive model gives an incorrect value of the ratio of the energies of different configurations; in comparison with the calculations, it seriously overestimates the ratio (5 instead of 2) of the energies of the linear and T-shaped configurations in the case in which the four centers coincide with the H atoms. If the distance between the four centers, r, is treated as an additional parameter of the model, then it is possible to reduce this discrepancy by reducing this distance with respect to the equilibrium distance r_e.

Yet another "refinement" of the additive model involved an attempt[23] to introduce an additional nonadditive component in expression (7); this new component would depend only on R. In a recent paper[23] on a nonempirical calculation of the potential-energy surface for the He–H_2 system at approach distances $R \sim r_e$, Russek and Ramiro Garcia[23] offered qualitative arguments in favor of this modification of the additive model. Their arguments, however, are seriously weakened by the fact that the modified potential-energy surface proposed in Ref. 23 fails to describe the differential-scattering pattern studied in Ref. 95.

b) Theoretical models for high-energy atom-molecule scattering

Direct quantum-mechanical solutions of the scattering problem are frequently difficult even for atom-atom sys-

tems. When the scattering involves molecules, there are, as yet, simply no alternatives to an approximate description. Let us examine the approximations which are being discussed in connection with the description of high-energy scattering.

1) *Classical approximation*. This is the most accessible analysis method, which is applicable to scattering through angles greater than the angle which bounds the zone of diffraction scattering and also to the multiquantum energy loss of molecules caused by collisions. The first step in this approximation is to calculate the trajectories[59] corresponding to fixed initial states of the molecule. The differential cross section is then found with respect to these states, and it is averaged over the set of initial states (usually by a Monte-Carlo method). These calculations are laborious, and it is customary to resort to further simplifications in the case of high-energy scattering. The first simplification is the approximation of rectilinear trajectories; the second is the approximation that the orientation and internuclear distance of the molecules are frozen during the collision.

The basic result of the numerical analysis of Ref. 96 of the effect of an anisotropy of the potential-energy surface in the classical approximation was the demonstration that the differential cross section averaged over the spatial orientations of the molecule is relatively insensitive to the anisotropy.

2) *Approximation of sudden perturbations*. This is the most popular quantum-mechanical approximation in the description of high-energy scattering.[97] In this approximation it is assumed that a molecule with a nonstationary initial state corresponding to a dumbbell in a rigid spatial orientation is scattered elastically. The decay time of this state is assumed to exceed the collision time. We denote by $f(\mathbf{r}, \mathbf{k} \to \mathbf{k}')$ the amplitude for this elastic scattering by an anisotropic potential, by $\mathbf{r}$ the vector internuclear distance of the molecule, and by $\mathbf{k}$ and $\mathbf{k}'$ the initial and final wave vectors ($|\mathbf{k}| = |\mathbf{k}'|$). The cross section for a transition between stationary states with given quantum numbers, $vjm \to v'j'm'$, is then given by

$$\sigma_{vjm\to v'j'm'}(\mathbf{k} \to \mathbf{k}') = \left| \int \psi^*_{vjm}(\mathbf{r}) f(\mathbf{r}, \mathbf{k} \to \mathbf{k}') \psi_{v'j'm'}(\mathbf{r})\, d\mathbf{r} \right|^2. \quad (8)$$

In this approximation, the differential cross section averaged over the final states, $\sigma_{vjm}(\mathbf{k} \to \mathbf{k}')$, is

$$\sigma_{vjm}(\mathbf{k} \to \mathbf{k}') = \sum_{v'j'm'} \sigma_{vjm\to v'j'm'}(\mathbf{k} \to \mathbf{k}') = \left| \int |\psi_v(r)|^2 f(\mathbf{r}, \mathbf{k} \to \mathbf{k}')\, dr \right|^2, \quad (9)$$

where $\psi_v(r)$ is the wave function of vibrational state v (in the approximation of an oscillating rotator) and is independent of the initial rotational state jm and of the change in r in the course of the collision. In addition, the ratio of the total cross sections for the rotational transitions, $\xi_{jj'}^{\Delta j}$, is independent of the energy:

$$\xi_{jj'}^{\Delta j} = \frac{Q^+(E,\ j \to j+\Delta j)}{Q^+(E,\ j' \to j'+\Delta j)} = \text{const}. \quad (10)$$

From the mathematical standpoint, the use of the approximation of sudden perturbations in the initial formulation reduces to the evaluation of multi-dimensional integrals of oscillatory functions—a problem which is overly time-consuming even for advanced computers. In practice, therefore, the so-called "approximation of sudden perturbations of infinite order" is used in the thermal energy range. In this approximation, the angle between the atom-molecule vector $\mathbf{R}$ and the axis of the molecule, $\mathbf{r}$, is assumed to remain fixed during the collision. In this case, $f(\mathbf{r}, \mathbf{k} \to \mathbf{k}')$ is calculated for an isotropic potential which depends parametrically on the angle.

Arguments have been raised against the use of the approximation of sudden perturbations for describing high-energy scattering.

3) *Semiclassical approximations*. The need to incorporate quantum effects in the analysis of inelastic rotational-vibrational transitions between low-lying quantum states has led to the development of a variety of semiclassical approximations. Apparently the most systematic of these approximations is the semiclassical scattering theory which uses action angle variables.[99] In this approach, the intramolecular motion in the course of the collision is taken into account, and it is possible in principle to incorporate both strong perturbations of the intramolecular motions on the trajectory and the effect on the dynamics. So far, however, the practical applications of this theory have used several simplifications, one being that the dynamic scattering pattern is assumed to be independent of the perturbation of the intramolecular motions of the projectile particle. The same limitation is inherent in the time-varying theories[100] in which the dynamic picture of the motion is calculated classically and without regard to the intramolecular motions, and then exact quantum-mechanical calculations are carried out on the evolution of the intramolecular states along the classical trajectory that has been obtained. Attempts are being made to incorporate in these models the inverse effect of the intramolecular motions on the scattering dynamics.[101]

4) *Distorted-wave approximation*. Measurements have shown (see Refs. 67 and 103, for example) that the differential cross sections for elastic scattering are substantially larger than those for inelastic transitions at small angles. It thus becomes possible to use (at least for a qualitative analysis) the distorted-wave approximation, in which the probability for a change in the initial state of the molecule $n\{v, j, m\}$, during the collision is assumed to be small. The first step is then to solve the problem for elastic scattering by a potential

$$V_{nn}(\mathbf{R}) = \langle \psi_n(\mathbf{r}) \mid V(\mathbf{R}, \mathbf{r}) \mid \psi_n(\mathbf{r}) \rangle \quad (11)$$

and to find the wave function for the elastic channel, $\varkappa_n(R)$. The scattering amplitude for inelastic transitions is determined by the integral

$$f_{n\to n'}(\mathbf{k}_n \to \mathbf{k}'_{n'}) = -\frac{\mu}{2\pi} \int e^{-i\mathbf{k}'_{n'}\mathbf{R}} V_{nn'}(\mathbf{R})\, \varkappa_n(\mathbf{R})\, d\mathbf{R}, \quad (12)$$

where $\mathbf{k}_n$ and $\mathbf{k}'_{n'}$ are the wave vectors of the initial and final channels, and $V_{nn}(\mathbf{R})$ are the matrix elements of the transitions between states n and n'. The methodological difficulty of the distorted-wave approximation is in choosing the ini-

tial state, since the elastic channel includes states with various projections (m) onto the quantization axis. It has been suggested[96] that as n we choose states vjm with quantization axis coinciding with the direction of the wave vector of the particle before the collision. In this case the entire problem of finding the transition amplitudes reduces to one of evaluating one-dimensional integrals. The cross section for depolarization (a change in m) for scattering through sufficiently small angles is small in this model.

In this version of the distorted-wave approximation, $\xi_{jj}^{\Delta j}$ is independent of E only in the limit $E \to \infty$. Important to an understanding of the sensitivity of the differential cross sections for the transitions to the shape of the potential-energy surface is an analysis of the matrix elements $V_{nn'}(\mathbf{R})$, which determine which components of the potential-energy surface contribute substantially to the cross section under consideration, $\sigma_{n \to n'}$ $(\mathbf{k}_n \to \mathbf{k}'_{n'})$. The results of this analysis which apply to the oscillating-rotator model are as follows. In the basis selected, the matrix elements are symmetric under rotation around the wave vector $\mathbf{k}_n$: $V_{nn}(\mathbf{R}) = V_{nn}(R, \mathbf{R}\mathbf{k}_n)$. In the semiclassical approximation we find an analog of the Moliere formula for the differential cross section for elastic scattering. The cross sections for rotational transitions are described by

$$\sigma_{\nu'jm \to \nu j'm'}(\theta_{\text{c.m.}}) = \left| 2\mu \int_0^\infty J_{|M|}(\theta_{\text{c.m.}} kb)\, b \left\{ \int_{-\infty}^{+\infty} \left[\sum_{l=0}^{L} \lambda_l P_l^{|M|}\left(\frac{z}{\sqrt{z^2+b^2}}\right) \times V_l^{\nu}\left(\sqrt{z^2+b^2}\right) \times \exp\left(i\Delta kz - \frac{i\mu}{k} \int_{-\infty}^{z} V_{\nu jm \to \nu jm}\, dz'\right)\right] dz \right\} db \right|^2, \quad (13)$$

where $M = m - m'$, $\Delta k \approx k(B/2E_{\text{c.m.}})(j' - j)(1 + j + j')$, the λ_l are the coefficients in the expansion of $V_{nn'}$ in Legendre polynomials, μ is the reduced mass of the molecule, b is the impact parameter, z is the coordinate of the translational motion of the atom, and B is the rotational constant. The subscript "c.m." means that the quantity refers to the center-of-mass system. For most molecules, B is small ($\sim 10^{-4}$ eV), and the phase shift (Δkz) over a distance of the order of the effective range of the potential is small. The only case in which this quantity is not small is that of hydrogen-like molecules in highly excited states (Δkz is not small for vibrational transitions and must be taken into account). In most cases, therefore, we can assume $\Delta k \approx 0$ for rotational transitions. For $j, j' \gg L$, the coefficients λ_l in (13) then depend only on the parameter $\eta = m/(j + 0.5)$ and the changes in quantum numbers Δj and Δm. In this case we have

$$\sigma_{\nu jm \to \nu' j'm'}(\theta_{\text{c.m.}}) = \sigma_\eta^{\nu, \Delta j, \Delta m}(\theta_{\text{c.m.}}). \quad (14)$$

We also note that the selection rule $|\Delta m| < l$ and the factor $J_{\Delta m}(kb\theta_{\text{c.m.}})$ in (13) lead to a relatively small change in m during the collision, since for $\Delta m \neq 0$ we have $J_{\Delta m}(x) \to 0$ as $x \to 0$ (small-angle scattering).

It follows that for $\nu 00 \to \nu jm$ transitions we would have $m = 0$ for the bulk of the scattered particles; i.e., the scattered flux would be polarized.

It follows that in the region in which the distorted-wave approximation is valid the differential cross sections for rotational transitions are the most convenient source of information on the anisotropy of the potential-energy surface, since scattering involving a change Δj in j is determined exclusively by the effective potential V_{nn} (found from data on elastic scattering) and the l-th component ($l = \Delta j$) of the expansion of the potential-energy suface in Legendre polynomials. Attempts to extract information on the anisotropy of the potential energy surface exclusively from data on elastic scattering will fail even in the case of a pronounced anisotropy, as numerical calculations have shown.[96]

Transitions involving a change in the vibrational number ν introduced a new feature: The anisotropic components of the expansion of the potential-energy surface in $(r - r_e)^p$ in the oscillating-rotator approximation are determined by rotational-vibrational transitions with $|\Delta\nu| = p$.

In summary, it may be said that the approximations which have been developed lead to a qualitative interpretation of the entire spectrum of phenomena observed in high-energy scattering. Their quantitative accuracy, on the other hand, is difficult to judge, so there is a need for the development of direct numerical methods for solving the multichannel problem of quantum scattering in this range of collision energies.

4. SUMMARY OF RESEARCH RESULTS ON HIGH-ENERGY SCATTERING

a) Elastic and molecular-inelastic scattering

In this section we consider the most important experimental results from research on high-energy scattering in the reduced-angle interval shown in Fig. 2. Since elastic scattering and molecular-inelastic scattering are most likely in this range, we would like to compare the results of measurements of the cross sections for these processes.

The integral cross sections for elastic scattering, $Q^-(E)$, and the cross sections for molecular transitions $Q^+(E)$ were

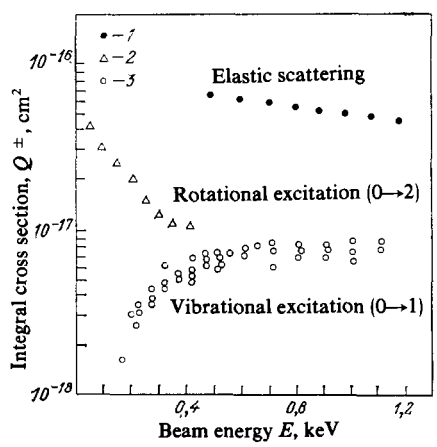

FIG. 8. Results of measurements of the integral cross sections in the Li^+–H_2 system. 1—Elastic scattering,[102] $Q^-(E)$; 2, 3—molecular transitions; 2—rotations[67]; 3—vibrations.[68]

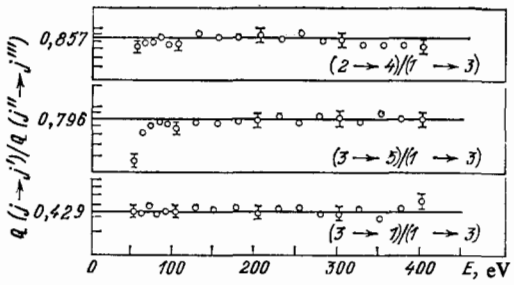

FIG. 9. Ratio of the integral cross sections Q^+ for rotational excitation and decay as a function of the collision energy E according to measurements for the Li^+–H_2 system in the apparatus in Fig. 3. The solid lines are values corresponding to ξ_B for various values of jj'.

measured in Refs. 67, 68, and 102. Figure 8 shows some typical results of measurements for the Li^+–H_2 system.

The first conclusion which can be drawn from the data in Fig. 8 is that the difference in the magnitudes of the cross sections allows us to ignore the mutual effects of the rotational excitation and vibrational excitation (this conclusion has been confirmed experimentally for He^+–N_2; Ref. 84), and we can also ignore the effect of these excitations on elastic scattering. This specific feature of high-energy scattering underlies the simplification of the theory for this scattering which we discussed above. Furthermore, the energy dependence of the partial transition cross sections might in principle be used to solve the inverse problem. The difficulties which arise here are consequences of the still imperfect methods for describing high-energy scattering. The implementation of these experimental possibilities will provide a stimulus for the development of a quantitative theory.

Itoh *et al.*[67] have recently measured the partial total cross sections $Q^+(E)$ for rotational transitions with $\Delta j = 2(\Delta j = j' - j$ for $j, j' \leqslant 5)$ for Li^+–H_2 collisions in the beam energy range 50–400 eV. They found that for the various values of j and j' the values of $\xi_{jj'}^{\Delta j}$ in (10) are constant for $E \geqslant 100$ eV, agreeing numerically with the value for the Born limit, ξ_B. At $E < 100$ eV there is a significant deviation from the Born limit (Fig. 9).

The reason for this deviation can be seen in the version of the distorted-wave approximation outlined above. In the basis selected, the expression for the transition cross section in (13) contains an oscillatory factor exp $(i\Delta kz)$, where $\Delta k \approx (B\mu/k)(1 + 2j + \Delta j)$.

In the high-energy limit we have $\Delta kz \to 0$, and the factor degenerates, while $\sigma_{vjm \to vj'm'}(\theta_{c.m.})$ depends only on $\Delta j = j - j =$ — not on the values of j and j' themselves (the Born limit for $j, j' \gg 1$). Under the condition $|\Delta kzR_{eff}| \gg 1$, where R_{eff} is the effective range of the potential, the exponential factor obviously leads to a decrease in the ratio of the cross sections, and we can use the estimate

$$\xi_{jj'}^{\Delta j} \approx \xi_B \frac{1+2j'+\Delta j}{1+2j+\Delta j}. \tag{15}$$

For $3 \to 5$ and $1 \to 3$ transitions (Fig. 9), expression (15) yields a value for $\xi_{jj'}^{\Delta j}$. which agrees with measurements at $E = 50$ eV. At $j > 3$, the distruption of the "frozen" condition is manifested at higher energies, and at $j = 10$, for example, we can expect to see deviations from the Born limit even at $E = 1000$ eV. Analogous effects should be observed for the ratios of the total cross sections of vibrational transitions.

Measurements of the integral cross sections for elastic scattering in atom-molecule and molecular systems have been used to determine the parameters of model potentials of the power-law[58] and exponential[59] types (for systems including molecules the potential has been assumed to be additive). The results of these studies are summarized in the review of Ref. 64. In the cases of ion-atom and ion-molecule systems (alkali ions and inert gas ions[74]), the integral cross sections have been measured[65,103] over a broad energy range, which has made it possible to span the interval of distances including the region of polarization attraction. A more flexible procedure has been used in some recent studies[65] to determine the potential from experimental data; in this procedure, it is possible to avoid *a priori* assumptions regarding the shape of the potential. In this case, a three-parameter approximation has been used for the dependence $\tau(b)$ of the reduced deflection angle. These parameter values are then varied to minimize the difference between the measured and calculated integral cross sections $Q^-(E)$. The deviation function $\tau(b)$ is then inverted directly, and a set of interaction energies is found for known internuclear distances.

There is a point to be noted in connection with empirical information on repulsive potentials for systems including molecules. In the theory of vibrational relaxation (see Ref. 104, for example), the probability for vibrational transitions is a sensitive function of the steepness of the potential. Consequently, there have been suggestions, dating back many years, that this characteristic might be determined from the temperature dependence of relaxation times.[105] As it turns out, however, the steepness of the potential found from the relaxation data agrees poorly with the results extracted from scattering data. This contradiction can be explained in part by the imperfections of the theory for impact excitation. Alternatively, this discrepancy might be attributed to the crudeness of the models which have been used for the potential-energy surfaces. These models can be refined by switching to measurements of the differential cross sections for elastic and molecular inelastic scattering.

Study of differential scattering in the diffraction region not only provides a high sensitivity to the fine structure of the potential but also offers the opportunity to increase substantially the information content of the experimental data. In contrast with the classical treatment of high-energy scattering, for quantum scattering the scattering patterns measured at various energies are not invariant when represented in terms of reduced angles and cross sections ($\tau = E\theta$, $\rho = \sigma\theta^2$). Consequently a variation of the beam energy provides an additional possibility for extracting information on the potential. That the structure can be resolved has been shown by recent studies of diffractive scattering with the help of a position-sensitive detectors.[106] Figure 10 shows the results of these measurements for the Li^+–N_2 system, along with calculations carried out for the nonempirical potential of Ref. 51. Comparison of the measured and calculated curves shows that even the combined effects of instrumental

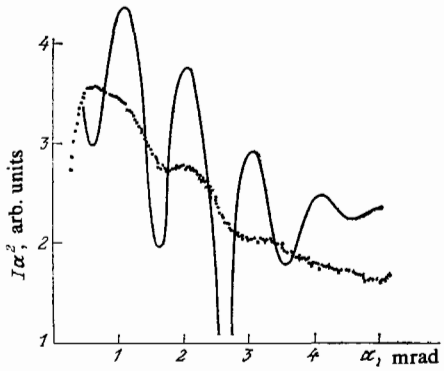

FIG. 10. First results of measurements of high-energy diffractive scattering in the Li^+–N_2 system by means of a position-sensitive detector.[81] Points—Measurements of Ref. 106; Solid line—calculated from the potential of Ref. 51.

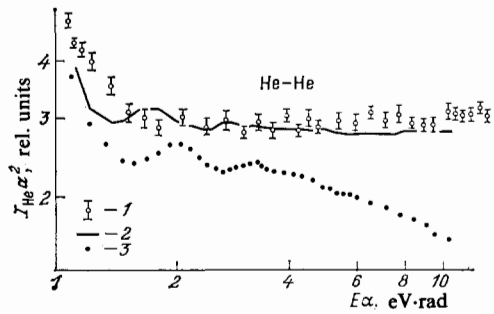

FIG. 11. Scattering pattern in the He-He system at $E = 600$ eV. 1—Measurements (the error bar shows the standard deviation); 2—result of a convolution of the cross section calculated in the semiclassical approximation with the selected interaction potential; 3—convolution of the cross section calculated from the theoretical potential of Ref. 108.

blurring (which can easily be reduced) and of an averaging over the orientations do not obliterate the diffraction structure. Furthermore, a comparison reveals a phase shift of the oscillations for the experimental and theoretical data, which is unambiguous evidence of a need for refining the theoretical potential. In a series of special model-based calculations[96] we have seen that the diffraction pattern of high-energy scattering (the frequency, phase, and amplitude of the oscillations) is quite sensitive to variations of the potential. It can thus be asserted that the present level of experimental methods and the development of suitable computational methods make it extremely promising to study the diffractive scattering of molecular systems.

The differential-scattering method has recently been used in very extensive studies of the repulsive interactions in atom-atom and atom-molecule systems (independent nonempirical calculations of the interaction energies have been carried out in parallel). In contrast with the thermal energy range, however, where the empirical potentials can be determined to within a few percent, and the results found from these potentials agree well with nonempirical calculations, at short and intermediate range the agreement between theoretical and experimental data is not as good.

This assertion is illustrated in Fig. 10 and also in Fig. 11, for the particular case of the He–He system. For this system, energy calculations have been carried out in more than ten studies (see the bibliography in Ref. 107). Figure 11 shows the experimental angular dependence $I(\alpha)\alpha^2/E\alpha$ for the scattering of a beam with $E = 600$ eV in a range of reduced angles $E\alpha$ corresponding to the interval of interaction energies 0.3–8 eV. Also shown here is the calculated functional dependence for the most reliable theoretical potential.[108] It can be seen from this comparison that even in this case—one of the simplest for quantum-chemistry calculations—the theoretical prediction of the scattering pattern deviates from the experimental results.

In order to resolve this discrepancy it was necessary to change the model potential. The empirical modification which resulted in agreement reduces to the introduction in the Born-Mayer potential of an additional, quadratic, dependence on the distance[109]: $V(R) = A\exp(-\alpha R - \beta R^2)$. The need for a modification of this type can also be seen in the other atomic and atom-molecule systems which have been studied. This modification is an important result, which absolutely must be taken into account in an analytic approximation of the results of theoretical calculations of interaction energies.

When we go from atom-atom to atom-molecule systems we find that the observed scattering pattern deviates even more from the pattern predicted on the basis of data from nonempirical calculations. Some typical experimental results are summarized in Fig. 12. In these measurements, along with the deviation of the functional dependence from that predicted for a simple exponential potential, we see the appearance of a structure scattering in the form of rainbow-

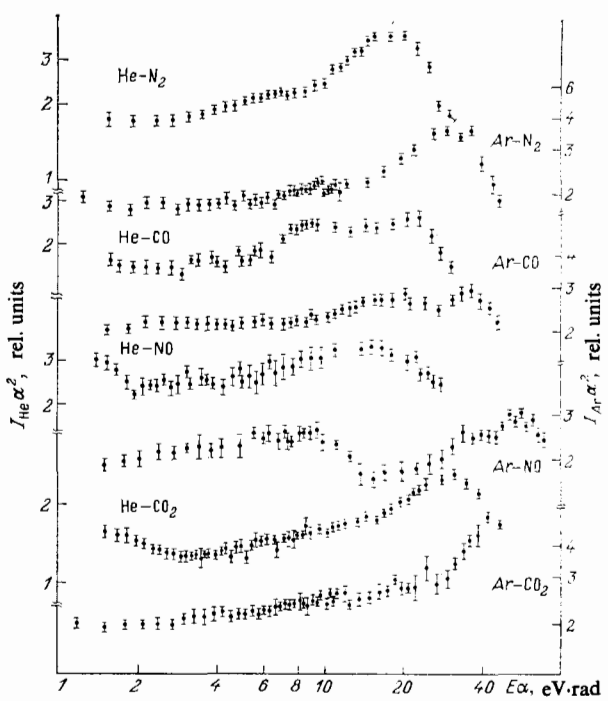

FIG. 12. Summary of the results of measurements of the differential scattering of atom-molecule systems.[112] Note the rainbow structure, which is not present in the case of atom-atom systems (see Ref. 11, for example).

like surges in the region $\alpha E \geqslant 15$ eV·rad. The discovery of a new (nondiffraction) structure in the scattering pattern is of fundamental importance to the solution of the inverse problem: that of reconstructing the multidimensional potential-energy surface from the measured differential cross sections.

Calculations of the high-energy scattering pattern which have been carried out for the He–H_2, H_2–H_2, Ar–CO, He–N_2, etc., systems[110] on the basis of the potential-energy surfaces (Table I) reveal significant discrepancies between the measured and calculated behavior. The nature of these discrepancies forces us to seek other sources of these features (sources other than imperfections of the radial dependence of the theoretical potential-energy surfaces). These other sources are discussed below.

b) The vibrational rainbow in high-energy scattering

Several measurements of the differential scattering of atom-molecule systems have revealed structural features of the rainbow type (Fig. 12), which are not found in the corresponding behavior for atom-atom scattering. Until very recently, the interpretation of molecular collisions under conditions of high-energy scattering was based exclusively on the representation of potential scattering with frozen intramolecular motions ($\mathbf{r} = \text{const}$). Consequently, when the structure was found an attempt was first made to link it to specific features of the potential-energy surfaces themselves. Since both the classical and quantum-mechanical calculations[96] carried out in the frozen-motion approximation indicate that the anisotropic components of the potential-energy surface should contribute little to the measured cross sections, it was assumed[111] that the effect might be due to the particular radial dependence of the spherically symmetric part of the overall potential-energy surface. However, it was quickly found that this assumption is artificial and we[96] offered a hypothesis to explain the observed structure. This hypothesis has the effect resulting from a pronounced perturbation of the intramolecular motion on the trajectory and the inverse influence of the perturbation on the collision dynamics. The effect was accordingly termed the "vibrational rainbow" in the high-energy scattering of molecules. The word "vibrational" emphasizes the fact that the effect stems primarily not from rotation but from a change in the intramolecular distance r, which is equivalent to a vibrational motion of the molecule. As part of this hypothesis it is assumed that the position of the maximum of the rainbow, τ_R, depends on the collision velocity u and on the initial vibrational state of the molecule, ν. An experimental test of these suggestions for the typical system He–N_2 (Fig. 13) confirmed[113,114] that the position of the rainbow peak, τ_R, does indeed depend on u ($\tau_R \sim u^{-1/2}$), and it revealed that the peak height decreases with the velocity. In experiments on scattering in the He–N_2 system it was found that interchanging the roles of the He and N_2 changes the observed scattering pattern. The population of the vibrational levels of N_2 molecules in a beam ($\nu \geqslant 1$) are different from those in a target ($\nu = 0$), since the beam is formed through electron-impact ionization, followed by a charge exchange of molecular ions. It is this difference in the vibrational state ν of the molecule

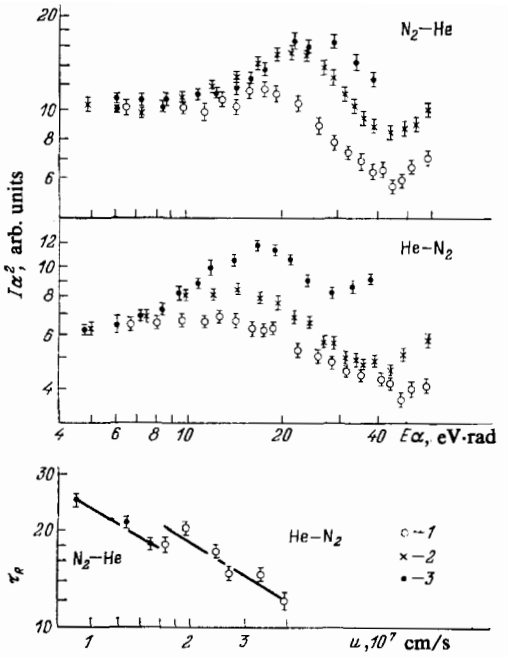

FIG. 13. Results of measurements[114] of the differential scattering in the He–N_2 system. The reduced intensity $I(\alpha)\alpha^2$ is shown as a function of the reduced angle $E\alpha$ for the scattering of a He beam in N_2 ($\nu_0 = 0$) and for the scattering of an N_2 beam in He ($\nu_0 \geqslant 1$). The energies of the scattered beams are (1) 3.2 keV, (2) 2.4 keV, and (3) 1.2 keV. Also shown here is the position of the rainbow peak, $\tau_R = E\alpha_R$ (eV·rad), as a function of the collision velocity u.

which explains the observed difference in scattering patterns (Fig. 13; it is necessary to compare the N_2–He scattering cross section at $E = 3200$ eV with the He–N_2 cross section for $E = 1200$ eV in order to deal with approximately the same collision velocity).

The experimental velocity dependence of τ_R allows us to reject immediately the possibility of explaining the effect on the basis of a specific nonmonotonic effective spherically symmetric potential or a dynamic manifestation of a crossing of quasimolecule terms of the ground and electronically excited states.

It can thus be concluded from the set of experimental data (Fig. 13) that the angular dependence $I(\alpha)$ is essentially multidimensional, $I = I(\alpha,\nu,u)$. This circumstance justifies the formulation of the problem of reconstructing a multidimensional potential-energy surface.

Following Ref. 115, we qualitatively analyze the vibrational-rainbow effect for the system consisting of an atom and a homonuclear diatomic molecule within the framework of classical mechanics. We describe the interaction by the model of a "breathing" sphere, $V(R,r)(= \langle V(\mathbf{R},\mathbf{r})\rangle)$ in which the initial surface is averaged over the spatial orientations of the molecule. We approximate the vibrations of the unperturbed molecule by the harmonic law $r(t) = \mathscr{A}\cos(\omega t + \varphi) + r_e$, where $\mathscr{A} = \sqrt{2(\nu + 0.5)/\mu\omega}$. In the approximation of a rectilinear ($\theta \ll 1$) trajectory, the reduced deflection function is

$$\tau(b, A, \varphi) = -\frac{1}{2}\int_{-\infty}^{+\infty}\left[\frac{b}{R}\frac{\partial}{\partial R}V(R, r(z, b, u, \mathscr{A}, \varphi))\right]_{R=\sqrt{b^2+z^2}} dz, \quad (16)$$

where the change in the internal coordinate r is described by

$$\frac{\partial^2 r}{\partial z^2} = -\frac{\omega^2}{u^2}(r-r_e) - \frac{1}{\mu u^2}\frac{\partial}{\partial r}V(\sqrt{b^2+z^2}, r) \quad (17)$$

($z = ut$, μ is the reduced mass of the molecule, and u is the collision velocity). Since the phase φ is not determined for an oscillator, the measured reduced cross section is an average over φ:

$$\rho(\tau, \nu) = \frac{\tau}{2\pi}\int_0^{2\pi} b(\tau, \nu, \varphi)\left|\frac{\partial b}{\partial \tau}\right| d\varphi. \quad (18)$$

We then have the standard formal condition for the appearance of a rainbow [i.e., the condition that $\rho(\tau, \nu)$ becomes infinite at $\tau = \tau_R$],

$$\left.\frac{\partial \tau}{\partial b}\right|_{\varphi=\varphi_R,\, b=b_R} = 0, \quad (19)$$

and the auxiliary condition

$$\left.\frac{\partial \tau}{\partial \varphi}\right|_{\varphi=\varphi_R,\, b=b_R} = 0.$$

Molecular scattering effects on the potential-energy surface are usually described through an expansion of the type

$$V(R, r) = V_0(R) + B(R)(r - r_e). \quad (20)$$

Using this expansion along with Eqs. (16) and (17) (and setting $\omega = \mathscr{A} = 0$), we find a relation for the reduced angle:

$$\tau(b) = \tau_0(b) + \frac{1}{\mu u^2}\Delta(b), \quad (21)$$

where $\tau_0(b)$ is determined by $V_0(R)$ [the first term in expansion (20)], $\Delta(b)$ is determined by $B(R)$ (the second term in the expansion), and we can use the estimates $\tau_0(b) \sim V_0(b)$ and $\Delta(b) \sim -B^2(b)R_{\text{eff}}^2$, where R_{eff} is the characteristic range of $V(R)$. As can be seen from (21), τ is an explicit function of the collision velocity. From the condition for the appearance of a rainbow, $\partial\tau/\partial b = 0$, we find the following relation (b_R is the impact parameter which corresponds to the rainbow angle τ_R):

$$B^2(b_R) \approx \frac{\mu u^2 V_0(b_R)}{R_{\text{eff}}^2}. \quad (22)$$

We can use (22) to find a numerical estimate of that value of $B(R)$ which would make possible an observable effect. Comparing this estimate with values found through analytic approximations of quantum-chemistry calculations (Table I), we see that the empirical estimate is five or ten times higher than the theoretical values. We thus have the problem of carrying out a more detailed study of the dependence of the potential-energy surface on the internal coordinates in quantum-chemistry calculations.

We have been discussing the simplest version of the analysis of the rainbow effect in high-energy scattering. In the next approximation we need to consider the effect of the initial vibrational state of the molecule. An initial vibrational excitation of the molecule makes it possible to find the dependence of the potential-energy surface on the internal coordinate over a broader range of this coordinate.

We recall that we are essentially using an effective spherically symmetric potential $V(R, r)$ in expression (20). Incorporating orientational effects results in nothing fundamentally new, but it should broaden and blur these rainbow structures.

The purpose of this qualitative discussion has been to demonstrate some possible approaches to the interpretation of the observed effect and for using it to obtain completely new information about potential-energy surfaces (sections of the surfaces along the coordinate r).

The quantitative results of the solution of the inverse problem are the attractive goal of further research in this direction, but the goal is still some distance away. Along the path to this goal lie the development of a quantum-mechanical theory of the inverse problem of the vibrational rainbow[116] and the acquisition of more extensive and more accurate experimental data, to the level required by these procedures.

c) Measurements of energy-loss spectra

A logical development in research on angular scattering is the measurement of double (angle-energy) differential scattering cross sections for atom-molecule systems. Ideally, such measurements, by providing information on the cross sections for transitions between distinct quantum states of molecules, would make it possible to reconstruct potential-energy surfaces of essentially any complexity. However, since technical capabilities are still far from ideal, a natural and reasonable compromise is to carry out angular measurements of the energy-loss spectra for various angular positions α. In practice, such measurements are carried out not

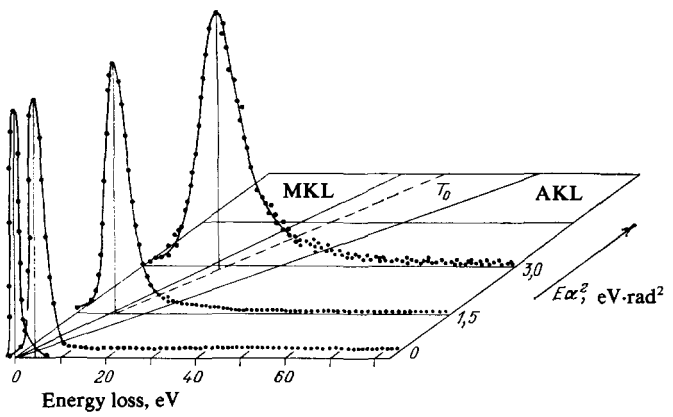

FIG. 14. Profiles of the energy-loss spectra of the Ne^+–D_2 system according to measurements in the scattering of a 3.5-keV beam of Ne^+ ions by a stationary target, for various angular positions α (Ref. 121). Also shown here are a plot of the most probable loss, T_0, versus $E\alpha^2$ (dashed line) and plots of the limiting energy loses in the models of molecular and atomic scattering (solid lines MKL and AKL). The molecular (MKL) and atomic (AKL) kinematic limits correspond to the losses in the laboratory coordinate system for the purely elastic scattering of the Ne^+ ion by a target particle with a mass $2M_D$ or M_D (M_D is the mass of the D atom), respectively.

in "lines" (i.e., not for the loss in transitions between known levels) but for unresolved bands, whose profiles may be linked with the most probable value of the loss due to internal excitation of molecular partners. Measurements using electrostatic analyzers in the case of the scattering of ions and using time-of-flight apparatus for neutral-atom beams have been carried out for the following systems: Li^+–N_2; He^+, Ar^+–N_2; Ne^+, Ne, D^+–H_2, D_2; He^+, He–H_2, O_2, N_2; and K^+, Cl^-–O_2, N_2, CO, CO_2, CH_4 (see the bibliographies in Refs. 84, 86, 117, and 118). Figure 14 shows some typical results for the Ne^+–D_2 system; shown along with the profiles of the measured-loss spectra here is the dependence of T_0—the most probable value of the loss (the peak in the spectrum)—on the reduced angle $E\alpha^2$. Also shown in Fig. 14 are the limiting values of the loss associated with purely elastic scattering: the lines labeled MKL (molecular kinematic elastic limit) and AKL (atomic kinematic elastic limit). These two limits have the following meaning. In the scattering of a fast atom (of mass M_P and energy E) by a molecular target (of mass M_T) which is at rest, the energy which the atom loses (and which is accordingly transferred to the target) in the laboratory coordinate system consists of two components. The component

$$\Delta E_\perp = \frac{\Delta P_\perp^2}{2M_T} = \frac{M_P}{M_T} E\theta^2 \approx \frac{M_P}{M_T} E\alpha^2$$

corresponds to the energy of the motion of the scattered molecule transverse with respect to the unperturbed trajectory. The other component, ΔE_{RV}, corresponds to the energy of the rotational-vibrational excitation of the molecule which arises. It is for the quantity $\Delta E_\perp$ that there are two limiting values (a molecular value and an atomic value), which depend on whether M_T arises as a unit (in which case we should have $M_T = \Sigma_i M_{\alpha_i}$, where M_{α_i} is the mass of the constituent atoms) or whether it may be thought of as a set of unbound atoms. In this case, in view of the short-range nature of the interaction, we would have $M_T = M_\alpha$. For a homonuclear diatomic molecule we would $M_\alpha \leqslant M_T \leqslant 2M_\alpha$. The intermediate cases which correspond to this inequality, and which are discussed on the basis of the scale transformation of the measurements for various values of E which was proposed in Ref. 119, correspond to scattering by an atom with an effective mass greater than M_α.

It can be seen from Fig. 14 that the measured loss spectra are characterized by a sharply defined peak T_0 and a significant broadening with increasing scattering angle. The angular dependence and the width of the loss spectrum are potentially sources of further information on the interaction potential in inelastic transitions. If we take T_0 to be the most probable value of the loss, then the difference $T_0 - E\alpha^2$ ($M_P = M_T$) corresponds to the energy of the rotational-vibrational excitation of the target molecule. In the additive-potential approximation it is a simple matter to calculate[59] T_0, by taking an average over random orientations of the loss $\Delta E_\perp$. Calculations of this sort have been carried out[86] in connection with measurements of the energy-loss spectra in the Li^+–N_2 system. Figure 15 shows measured and calculated values of T_0 (the circles and the solid line, respectively). The other lines shown here correspond to the molecular and

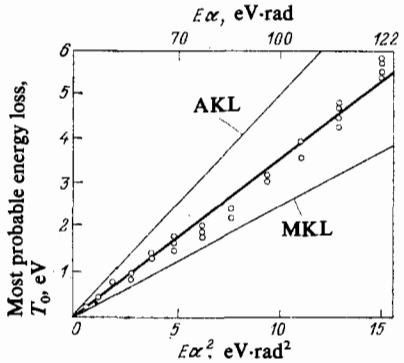

FIG. 15. The most probable energy loss, T_0, measured for the Li^+–N_2 system[86] versus $E\alpha^2$ and [$E\alpha \mid \propto V(b)$]. The limiting lines MKL and AKL are also shown. The difference between the values of T_0 and the values for the MKL line is a measure of the total loss due to molecular excitation.

atomic limits. As expected, the pulse mechanism for the excitation of the molecules, which gives a satisfactory description of the measured angular variation of T_0 (Fig. 15), leads to relatively small excitations ($\Delta E_{RV} \ll \tau$) up to $\tau \sim 50$ eV·rad.

Although the additive potential model also gives a satisfactory description of the angular dependence of T_0, the calculated results are not adequately sensitive to the potential. For collisions in, again, the Li^+–N_2 system, for example, with energies ~ 10 eV (Ref. 120), the loss spectra measured by Toennies *et al.*[120] can be described satisfactorily by using different values for the parameters of the Born-Mayer potential for interatomic repulsion

$$V(R) = A \exp(-\alpha R)$$

($A = 3563$ eV $\alpha = 3.78$ Å^{-1} [120];
$A = 1550$ eV $\alpha = 4.65$ Å^{-1} [86]).

So far, the possibility of obtaining information on the potential-energy surface by fitting the calculated and measured shapes of the loss spectrum (going beyond a simple fit of the values of T_0) has not yet been pursued. This approach in the analysis of measurements of the overall profile of the energy-loss spectra appears to us to be more promising than the simple scale transformation of the experimental results which has been proposed by Sigmund[119] and which leads to a purely qualitative phenomenological result: the determination of some effective mass of the scatterer. As support for this position we can cite the results of recent measurements of the angular dependence of the loss spectra in the scattering of the electronically similar ions K^+ and Cl^- by different molecules (O_2, N_2, CO, CO_2, CH_4). The use of a scale transformation has not made it possible to extract anything in the way of practically useful information on the nature of the interaction responsible for the scattering at energies $V(R) \leqslant 10$–15 eV.

It is easy to see from Fig. 14 that the observed degree of broadening of the spectrum and the tendency for the width to increase with the scattering angle cannot be explained as purely instrumental effects (the role of such effects would weaken with increasing angle). The relative width of the loss spectrum, $\sigma T/T$, is determined by the interval of angles de-

tected by the detector, by the spread of initial energies in the beam and, finally, by the spread in the values of the effective mass M due to the orientation, as was shown in Ref. 117. All these contributions to the broadening of the spectrum should decrease with increasing angle, leading to a relative width $\sigma T/T \approx 0.1$. It can be seen from Fig. 14, however, that at the end of the angular interval of the measurements we have $\sigma T/T \approx 0.5$, indicating additional sources of broadening of the energy-loss spectra. At intermediate angles (Fig. 14) we also see indications of an additional source of broadening. Calculations in the impulse approximation show that the loss due to the vibrational-rotational excitation is a small fraction of the atomic kinematic limit. For the Ne^+–D_2 system, therefore, the energy transfer to the vibrational-rotational motion is $\Delta E_{RV} < 0.5E\alpha^2$. We then see from Fig. 14 that in essentially all cases the width of the loss spectrum is several times greater than ΔE_{RV}. The reason for this broadening should apparently be sought in the possibility that other sources of vibrational excitation come into play, in particular, sources associated with the observation of a strong dependence of the potential-energy surface on the internal coordinate, discussed above.

In summary, further developments in research and a more profound analysis of the angular dependence of the energy-loss spectra appear quite promising for obtaining new information on both the repulsive interaction and the loss function $\Delta E_{RV}(\theta)$.

5. CONCLUSION

This discussion of the present state of research on short-range intermolecular forces can be summarized as follows:

a) There is increasing interest in the use of data on interaction potentials, since this fundamental information makes it possible not only to find a quantitative description of collisional processes but also to avoid effectively the insurmountable difficulties in a direct determination of the macroscopic properties of matter under extreme conditions.

b) A computational branch of quantum chemistry has been defined and is being developed actively. This branch is presenting some impressive opportunities for calculations on short-range anisotropic interaction potentials. The reason for the interest in empirical data on the potentials here stems from the need to develop and test new approximations and new computational methods.

c) Extensive research has been carried out on high-energy scattering in systems including atoms, ions, and molecules. This research has provided voluminous empirical information on the potential-energy surfaces. A new phenomenon has been discovered: the high-energy vibrational rainbow. The possibility of obtaining fundamentally new information—sections of potential-energy surfaces along the intramolecular coordinate—is linked with the study of this rainbow.

d) The arsenal of experimental methods for studying high-energy scattering is expanding at a rapid pace. Position-sensitive detectors and laser methods are the most promising directions.

On the whole, this branch of the physics of atomic collisions has now reached a critical point of a sort, at which we are stepping from a region of methodological development into a region of acquiring reliable quantitative data on short-range interactions in atom-molecule systems.

[1]D. R. Bates (editor), *Atomic and Molecular Processes*, Academic, Orlando, 1962 (Russ. Transl., Mir, M., 1964).
[2]A. V. Bushman and V. E. Fortov, Usp. Fiz. Nauk **140**, 177 (1983) [Sov. Phys. Usp. **26**, 465 (1983)].
[3]W. J. Nellis, M. van Thiel, and A. C. Mitchell, Phys. Rev. Lett. **48**, 816 (1982).
[4]K. I. Kondo and T. J. Ahrens, Geophys. Res. Lett. **10**, 281 (1983).
[5]F. H. Ree, Preprint UCRL-85783, Livermore Laboratory, 1980.
[6]J. L. Lebowitz and J. K. Percus, J. Chem. Phys. **79**, 443 (1983).
[7]V. B. Leonas and A. V. Sermyagin, Pis'ma Zh. Eksp. Teor. Fiz. **12**, 432 (1970) [JETP Lett. **12**, 300 (1970)].
[8]N. N. Kalitkin and L. V. Kuz'mina, Fiz. Plazmy **2**, 858 (1976) [Sov. J. Plasma Phys. **2**, 478 (1976)].
[9]H. F. Schaefer, in: *Atom-Molecule Collision Theory* (ed. R. B. Bernstein), Plenum Press, New York, 1980, p. 111.
[10]V. K. Nikulin and Yu. N. Tsarev, Chem. Phys. **10**, 433 (1975).
[11]M. Ross, F. H. Ree, and D. A. Young, J. Chem. Phys. **79**, 1487 (1983).
[12]D. R. Flower *et al.*, Chem. Phys. **37**, 555 (1979).
[13]M. C. Hemert, J. Chem. Phys. **78**, 2345 (1983).
[14]N. Sathyamurthy and L. M. Raff, J. Chem. Phys. **66**, 2191 (1977).
[15]D. R. Yarkony, J. Chem. Phys. **60**, 856 (1974).
[16]F. H. Ree and N. W. Winter, J. Chem. Phys. **73**, 322 (1980).
[17]S. W. Harrison *et al.*, Int. J. Quantum Chem. **14**, 319 (1978).
[18]W. Kołos *et al.*, Int. J. Quantum Chem. **17**, 429 (1980).
[19]P. Siegbahn *et al.*, J. Chem. Phys. **68**, 2457, 2466 (1978).
[20]Sh. Green and P. Thaddeus, Astrophys. J. **205**, 766 (1976).
[21]A. W. Rakzkowski and W. A. Lester, Jr., Chem. Phys. Lett. **47**, 45 (1977).
[22]W. Mayer *et al.*, J. Chem. Phys. **73**, 1880 (1980).
[23]A. Russek and R. Ramiro Garcia, Phys. Rev. **A26**, 1924 (1982).
[24]J. Dietrich and R. W. Conn, J. Chem. Phys. **64**, 3091 (1975).
[25]D. M. Silver, J. Chem. Phys. **72**, 6445 (1980).
[26]V. I. Gaĭdaenko and M. N. Kuznetsov, Zh. Tekh. Fiz. **46**, 852 (1976) [Sov. Phys. Tech. Phys. **21**, 493 (1976)].
[27]L. D. Thomas *et al.*, Chem. Phys. **51**, 131 (1980).
[28]Sh. Green and P. Thaddeus, Astrophys. J. **206**, 766 (1976).
[29]Sh. Green and L. Monchick, J. Chem. Phys. **63**, 4198 (1975).
[30]Sh. Green and P. Thaddeus, Astrophys. J. **191**, 653 (1974).
[31]G. A. Parker *et al.*, J. Chem. Phys. **64**, 1668 (1976).
[32]C. L. Stroud and L. M. Raff, J. Chem. Phys. **72**, 5479 (1980).
[33]Sh. Green, J. Chem. Phys. **64**, 3463 (1976).
[34]S. L. Davis, J. Chem. Phys. **71**, 1418 (1979).
[35]Sh. Green *et al.*, J. Chem. Phys. **63**, 1154 (1975).
[36]J. Romelt *et al.*, Chem. Phys. **34**, 403 (1978).
[37]J. W. Birks *et al.*, J. Chem. Phys. **63**, 1741 (1975).
[38]S. Odiot *et al.*, Chem. Phys. Lett. **71**, 307 (1980).
[39]G. D. Billing, Chem. Phys. Lett. **71**, 255 (1980).
[40]N. C. Blais and D. G. Truhlar, J. Chem. Phys. **65**, 5335 (1976).
[41]G. A. Parker and R. T. Pack, J. Chem. Phys. **69**, 3268 (1978).
[42]Y. S. Kim, J. Chem. Phys. **68**, 5001 (1978).
[43]G. C. Nielsen, J. Chem. Phys. **66**, 1396 (1977).
[44]R. K. Preston and R. T. Pack, J. Chem. Phys,. **66**, 2480 (1977).
[45]Sh. Green, J. Chem. Phys. **60**, 2654 (1974).
[46]J. M. Murrel, Mol. Phys. **42**, 605 (1981).
[47]A. F. Wagner *et al.*, J. Chem. Phys. **69**, 3756 (1978).
[48]R. Schinke *et al.*, J. Chem. Phys. **74**, 3916 (1981).
[49]R. Schinke *et al.*, J. Chem. Phys. **72**, 3909 (1980).
[50]W. A. Lester, Jr., J. Chem. Phys. **54**, 3171 (1971).
[51]V. Staemler, Chem. Phys. **7**, 17 (1975).
[52]G. A. Pfeffer and D. Secrest, J. Chem. Phys. **78**, 3052 (1983).
[53]F. A. Gianturco *et al.*, Chem. Phys. **48**, 387 (1980).
[54]E. Clementi and H. Porkie, J. Chem. Phys. **57**, 1077 (1972).
[55]M. D. Dolgushin and N. N. Makovskiĭ, Preprint ITF-77-128R, Kiev, 1977.
[56]Sh. Green, Astrophys. J. **201**, 366 (1975).
[57]I. Amdur and H. Pearlman, J. Chem. Phys. **9**, 503 (1941).
[58]I. Amdur and J. Jordan, in: Research Using Molecular Beams (Russ. Transl., ed. A. M. Brodskiĭ and V. B. Leonas, Mir, M. 1969, p. 39).
[59]V. B. Leonas, Usp. Fiz. Nauk **107**, 29 (1972) [Sov. Phys. Usp. **15**, 266 (1972)].

[60]A. V. Eletskiĭ, L. A. Galkina, and B. M. Smirnov, Yavleniya perenosa v slaboionizovannoĭ plazme (Transport Phenomena in Weakly Ionized Plasmas), Atomizdat, Moscow, 1975.
[61]V. B. Leonas, in: Khimiya plazmy (Plasma Chemistry) (ed. B. M. Smirnov), No. 1, Atomizdat, M., 1974, p. 234.
[62]P. Kush, J. Chem. Phys. **40**, 1 (1964).
[63]A. P. Kalinin *et al.*, Vestn. Mosk. Univ. Fiz. Astron. No. 3, 245 (1971).
[64]V. B. Leonas, Mezhmolekulyarnye vzaimodeĭstviya i stolknoveniya atomov i molekul (Intermolecular Interactions and Collisions of Atoms and Molecules), VINITI, M. 1980.
[65]P. Polak-Dingels, M. S. Rajan, and E. A. Gislason, J. Chem. Phys. **77**, 3983 (1982).
[66]V. I. Chigin', Author's Abstract, Candidate's Dissertation, LGU, L'vov, 1982.
[67]Y. Itoh, N. Kobayashi, and Y. Kaneko, J. Phys. B **14**, 679 (1981).
[68]N. Kobayashi, H. Itoh, and Y. Kaneko, J. Phys. Soc. Jpn. **46**, 208 (1979).
[69]H. Itoh, N. Kobayashi, and Y. Kaneko, J. Phys. Soc. Jpn. **51**, 2977 (1982).
[70]J. C. Brenot, J. Pommier, and M. Barat, J. Phys. B **8**, 448 (1975).
[71]W. L. Hodge *et al.*, Phys. Rev. **A16**, 2360 (1977).
[72]Y. Itoh, N. Kobayashi, and Y. Kaneko, J. Phys. Soc. Jpn. **51**, 2977 (1982).
[73]A. P. Kalinin and V. B. Leonas, Dokl. Akad. Nauk SSSR **261**, 1113 (1981) [Sov. Phys. Dokl. **26**, 1147 (1981)].
[74]H. Inouye and R. Tanji-Noda, J. Chem. Phys. **77**, 5990 (1982).
[75]B. V. Zubkov, A. P. Kalinin, and V. B. Leonas, Prib. Tekh. Eksp. No. **4**, 201 (1977).
[76]M. A. Gruntman, Preprint IKI AN SSSR PR-701, Moscow, 1982.
[77]R. W. Wijnaendts van Resandt and J. Los, in: Proceedings of the Eleventh International Conference on Physics of Electronic and Atomic Collisions, Kyoto, 1979, p. 163.
[78]M. R. Aĭnbund *et al.*, Preprint IKI AN SSSR PR-787, Moscow, 1983.
[79]V. B. Leonas, Usp. Fiz. Nauk **127**, 319 (1979) [Sov. Phys. Usp. **22**, 109 (1979)].
[80]Y. S. Chen, J. N. Newman, K. A. Smith, and R. F. Stebbings, Bull. Am. Phys. Soc. **2**, 777, 805 (1983).
[81]R. W. Wijnaendts van Resandt *et al.*, Chem. Phys. **2**, 151 (1978).
[82]J. Hermann *et al.*, J. Phys. B **13**, L165 (1976).
[83]K.-I. Niurao and H. Inouye, J. Phys. Soc. Jpn. **40**, 813 (1976).
[84]D. Dowek *et al.*, Phys. Rev. A **24**, 2445 (1981).
[85]A. Lebehot and R. Campargue, J. Phys. B **15**, 1711 (1982).
[86]Y. Sato, K. Niurao, H. Takagi, and H. Inouye, J. Chem. Phys. **65**, 3952 (1976).
[87]N. Andersen, M. Vedder, A. Russek, and E. Pollak, J. Phys. V **11**, L493 (1978).
[88]V. B. Leonas and I. D. Rodionov, Preprint IKI AN SSSR PR-703, Moscow, 1982.
[89]K. Bergman, U. Hefter, and J. Witt, J. Chem. Phys. **9**, 4777 (1980).
[90]A. Ding and K. Richter, Z. Phys. A **307**, 31 (1982).
[91]D. A. Badalyan, Izv. Akad. Nauk Arm. SSR Fiz. **17**, 322 (1982).
[92]V. B. Leonas and I. D. Rodionov, Comm. At. Mol. Phys. **14**, 1 (1983).
[93]P. A. Monson and W. A. Steele, Mol. Phys. **49**, 253 (1983).
[94]A. K. McMahan *et al.*, Phys. Rev. A **9**, 1852 (1974).
[95]V. B. Leonas and A. V. Sermyagin, Khim. Vys. Énerg. No. 5, 296 (1977).
[96]V. B. Leonas and I. D. Rodionov, Preprint IKI AN SSSR PR-698, Moscow, 1982.
[97]D. M. Chase, Phys. Rev. **104**, 838 (1956).
[98]V. B. Leonas and I. D. Rodionov, in: Thirteenth RGD Symposium, Novosibirsk, July 5-9, 1982; Books of Abstracts Vol. 1, 1982, p. 288.
[99]A. V. Bogdanov, Supplement to: F. O. Goodman and H. Y. Wachman, Dynamics of Gas-Surface Scattering, Academic, Orlando, 1976 (Russ. Transl., ed. R. G. Barantsev, Mir. M., 1980).
[100]A. S. Dickinson, in: Semiclassical Methods in Molecular Collisions (ed. M. S. Child), D. Reidel, Dordrecht, Holland, 1980, p. 263.
[101]G. D. Billing, Chem. Phys. **65**, 323 (1982).
[102]H. Inouye and S. Kita, J. Chem. Phys. **59**, 6656 (1973).
[103]M. S. Rajan and E. A. Gislason, J. Chem. Phys. **78**, 2428 (1983).
[104]C. D. Clary, Mol. Phys. **39**, 1295 (1980).
[105]E. V. Stupochenko, S. A. Losev, and A. I. Osipov, Relaksatsionnye protsessy v udarnykh volnakh (Relaxation Processes in Shock Waves), Nauka, Moscow, 1965.
[106]A. P. Kalinin *et al.*, Chem. Phys. **83**, 341 (1984).
[107]D. M. Silver, Phys. Rev. A **21**, 1106 (1980).
[108]D. J. Klein *et al.*, J. Chem. Phys. **47**, 4862 (1967).
[109]V. N. Khromov and V. B. Leonas, in: Sixth International Conference on Atomic Physics; Abstracts of Contributed Papers, Riga, 1978, p. 283.
[110]V. N. Khromov and V. B. Leonas, J. Phys. B **12**, 219 (1979).
[111]A. P. Kalinin, Zh. Tekh. Fiz. **52**, 549 (1982) [Sov. Phys. Tech. Phys. **27**, 354 (1982)].
[112]A. P. Kalinin, V. N. Khromov, and V. B. Leonas, Mol. Phys. **47**, 811 (1982).
[113]A. P. Kalinin, V. B. Leonas, and I. D. Rodionov, Dokl. Akad. Nauk SSSR **268**, 347 (1983) [Sov. Phys. Dokl. **28**, 39 (1983)].
[114]A. P. Kalinin and V. B. Leonas, in: Ninth International Symposium on Molecular Beams; Book of Extended Abstracts, Freiburg, 1983, p. 249.
[115]I. D. Rodionov, Preprint IP-189, Institute of Applied Mathematics, Academy of Sciences of the USSR, Moscow, 1982.
[116]I. D. Rodionov, Preprint IP-7, Institute of Applied Mathematics, Academy of Sciences of the USSR, Moscow, 1983.
[117]R. Snyder and A. Russek, Phys. Rev. **A26**, 1931 (1982).
[118]M. Vedder, J. Phys. B **15**, 4411 (1982).
[119]P. Sigmund, J. Phys. B **14**, L321 (1981).
[120]R. Bottner, U. Ross, and J. P. Toennies, J. Chem. Phys. **65**, 733 (1976).
[121]N. Andersen, M. Vedder, A. Russek, and E. Pollack, Phys. Rev. A **21**, 782 (1980).
[122]B. V. Zubkov and A. P. Kalinin, Preprint IKI AN SSR PR-822, Moscow, 1983.

Translated by Dave Parsons